

Effect of Diffusion Time on Diffusion Kurtosis in Neural Tissues

E. S. Hui^{1,2}, S. H. Fung^{2,3}, and E. X. Wu^{1,4}

¹Laboratory of Biomedical Imaging and Signal Processing, The University of Hong Kong, Hong Kong, Hong Kong, ²Department of Radiology Research, The Methodist Hospital Research Institute, Houston, Texas, United States, ³Department of Radiology, Weill Medical College of Cornell University, New York, New York, United States, ⁴Department of Electrical & Electronic Engineering, The University of Hong Kong, Hong Kong, Hong Kong

Introduction Complex cellular microstructures in biological tissues hinder and restrict water molecule diffusion, leading to non-monoexponential dependence of diffusion-weighted (DW) signal on b-value. Various approaches, namely bi-exponential model (1), q-space imaging (QSI) (2), stretched-exponential model (3), and higher order or generalized diffusion tensor approaches (4, 5), have been proposed to explore such non-monoexponentiality of DW signal in neural tissues. In fact, DW signal attenuation not only depends on diffusion gradient strength but also the time separation between the 2 diffusion gradients (i.e., diffusion time Δ). It has previously been shown in QSI experiments that the water displacement profile varies with Δ to different extent in different neural structures (6, 7). However, a major drawback of QSI is the limited diffusion encoding directions, typically parallel or perpendicular to the long axis of axons (6, 8), causing neural tissue characterization difficult when there is no predomination diffusion direction. Another limitation is that very high b-value is typically used, and it results in very poor signal-to-noise ratio (SNR) in DW images (DWIs) (9). Recently, a more robust and efficient characterization of diffusion restriction in tissue microstructure has been made demonstrated by diffusion kurtosis imaging (DKI) (10-12). DKI quantifies both diffusivity (characterized by a 2nd order 3D diffusivity tensor as in conventional DTI) and diffusion kurtosis of the water diffusion profile (characterized by a 4th order 3D kurtosis tensor). In this study, we aimed to examine the effect of Δ on diffusion kurtosis quantitation by acquiring and analyzing the DW signals at multiple b-values and with different diffusion times in rat brains in vivo.

Methods All in vivo experiments were performed using a Bruker 7T scanner on normal adult SD rats (N=4). DWIs with 4 different b-values (0.5, 1.25, 2, 2.5ms/ μm^2) along 15 gradient encoding directions were acquired with a respiration-gated 2-shot stimulated-echo-EPI sequence. The DW experiments were repeated with $\Delta=40, 70, 95, 125, 150, 190\text{ms}$. The imaging parameters were TR/TE=3000/25.1ms, $\delta=6\text{ms}$, slice thickness=1.2mm, FOV=60x40mm², data matrix=96x64 (zero-filled to 128x128) and NEX=2. DWIs were first coregistered using AIR5.2.5. DW signals as a function of b-value for each Δ are fitted to the DKI model $\ln(S/S_0) = -bD + (1/6)b^2D^2K$, and apparent diffusion coefficient (D) and diffusion kurtosis (K) along each direction are then obtained (11). A key DKI parameter, mean kurtosis (MK) computed as the average of K along all encoding directions (11), was quantified as a function of Δ . In addition, mean diffusivity (MD), fractional anisotropy (FA) and directional diffusivity maps were computed from the diffusivity tensor. Multi-slice region-of-interests (ROIs), 2 white matter (WM) structures, corpus callosum (CC, 44 \pm 5 pixels) and internal capsule (IC, 20 \pm 5), and 3 gray matter (GM) structures, cortex (CT, 768 \pm 107), hippocampus (HP, 30 \pm 2) and caudate putamen (CU, 111 \pm 11), were defined in the FA and radial diffusivity λ_{\perp} maps as previously described (10, 12). These ROIs are illustrated in Fig.1.

Results Typical log mean DW (mDW) signal decays from an animal, computed as the average of all normalized DW signals along 15 encoding directions vs. b-value at different Δ , are shown in Fig.2 for different structures. It can be observed that mDW signal decays in WM structures increased with Δ , with IC showing the larger spread. In GM structures, signal decays were minimally affected by different Δ values studied. The corresponding ROI quantifications of MK, MD and FA from all animals are shown in Fig.3. MK decreased and then plateaued with Δ in all structures except IC, whereas a generally decreasing and increasing trend existed for MD and FA, respectively, in all structures. Noted that FA and MD computed by fitting all multiple-b-value DWIs to the monoexponential DTI model (in contrast to DKI model) showed similar trends to those obtained from DKI model (data not shown).

Discussions and Conclusions The drop in MD with Δ is expected because the probability for water molecule to encounter diffusion barrier would increase with Δ . Furthermore, MK in all structures (except IC) was seen to decrease and then plateau with Δ . First, the fact that MK at $\Delta=190\text{ms}$ was at least 80% of that of $\Delta=40\text{ms}$ in all structures suggests the existence of significant diffusion restriction at $\Delta=190\text{ms}$. Note that the MK decrease with Δ is counter-intuitive as one might expect the kurtosis to increase with Δ because apparent diffusion restriction can increase with increased diffusion distance during measurement time. However, one may also argue that long diffusion distance can average out the diffusion restriction effect within the microscopically inhomogeneous microstructures. Secondly, MK gradually plateaued with Δ . This might be explained by the increasing role of water exchange across cellular membranes. When Δ approaches the exchange time, the apparent diffusion restriction effect will diminish, leading to decrease of diffusion kurtosis observed in DKI. Lastly, the percentage change of MK with respect to Δ was observed to vary among different structures. One may speculate that such variations are associated with the specific cellular dimension, rate of water exchange across membrane, and intra- and extracellular diffusivities in a particular tissue structure. Furthermore, how MK depends on Δ may provide insights into these cellular properties. In summary, the current study has documented the DW signal decays with respect to Δ . The dependence of diffusion kurtosis on Δ has been examined in vivo for the first time, demonstrating the effect of Δ in kurtosis quantification in various neural tissues.

References: 1. Mulkern et al., NMR Biomed 12 (1999). 2. Callaghan. Oxford University Press (1991). 3. Bennett et al., MRM 50 (2003). 4. Liu et al., MRM 51 (2004). 5. Ozarslan et al., MRM 50 (2003). 6. Assaf et al., MRM 43 (2000). 7. Cohen et al., NMR Biomed 15 (2002). 8. Bar-Shir et al., NMR Biomed 21 (2008). 9. Jones et al., MRM 52 (2004). 10. Hui et al., Neuroimage 42 (2008). 11. Jensen et al., MRM 53 (2005). 12. Cheung et al., Neuroimage 45 (2009).

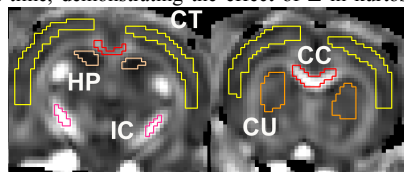


Fig.1 ROI definitions. CC: Corpus callosum, IC: internal capsule, CT: cortex, HP: hippocampus, CU: caudate putamen.

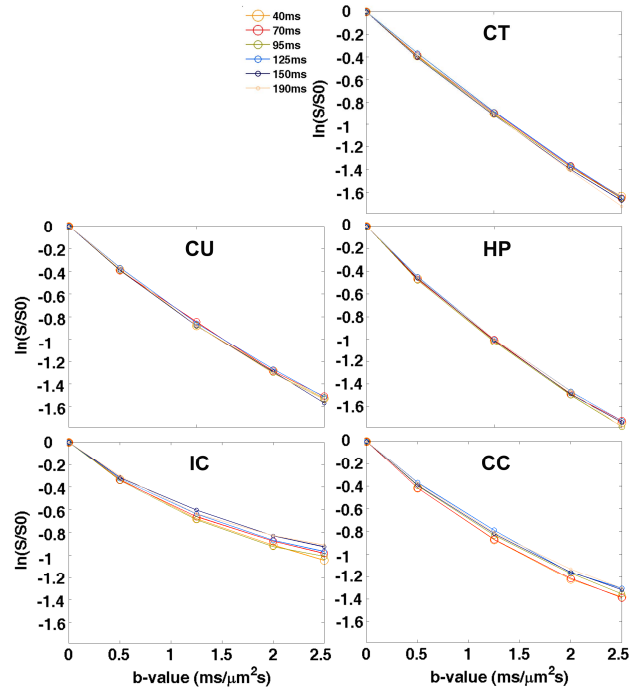


Fig.2 Log mean DW (mDW) signal decays, computed as the average of all DW signal along 15 encoding directions, vs. b-value at different Δ for all structures.

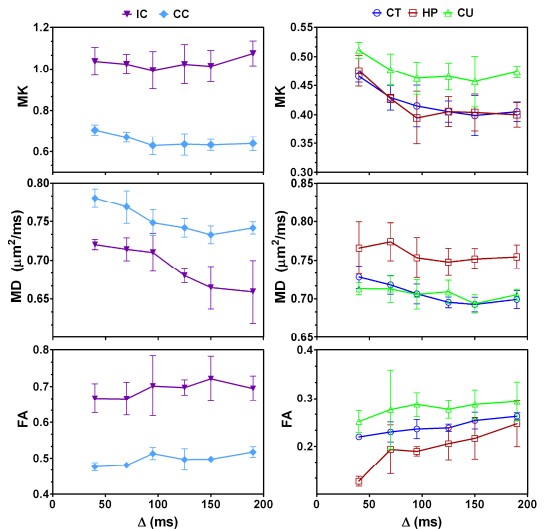


Fig.3 ROI quantifications of MK, MD and FA obtained from DKI model in all animals (N=4) vs. Δ . The error bar indicates the SD of measurement across all animals.